Establishment and evaluation of an automatic multi-sequence MRI segmentation model of primary central nervous system lymphoma based on the nnU-Net deep learning network method

TAO WANG[1*], XINGRU TANG[2*], JUN DU[3], YONGQIAN JIA[1], WEIWEI MOU[4] and GUANG LU[5]

[1]Department of Hematology, West China Hospital, Sichuan University, Chengdu, Sichuan 610041, P.R. China;
[2]Department of Clinical Medicine, Shanghai Jiao Tong University, Shanghai 200030, P.R. China;
[3]Department of Hematology, Shanghai Jiao Tong University School of Medicine Affiliated Renji Hospital, Shanghai 200001, P.R. China;
[4]Department of Pediatrics, Shengli Oilfield Central Hospital, Dongying, Shandong 257099, P.R. China;
[5]Department of Hematology, Shandong Second Provincial General Hospital, Jinan, Shandong 250022, P.R. China

Received November 8, 2024; Accepted April 8, 2025

DOI: 10.3892/ol.2025.15080

Abstract. Accurate quantitative assessment using gadolinium-contrast magnetic resonance imaging (MRI) is crucial in therapy planning, surveillance and prognostic assessment of primary central nervous system lymphoma (PCNSL). The present study aimed to develop a multimodal artificial intelligence deep learning segmentation model to address the challenges associated with traditional 2D measurements and manual volume assessments in MRI. Data from 49 pathologically-confirmed patients with PCNSL from six Chinese medical centers were analyzed, and regions of interest were manually segmented on contrast-enhanced T1-weighted and T2-weighted MRI scans for each patient, followed by fully automated voxel-wise segmentation of tumor components using a 3-dimenstional convolutional deep neural network. Furthermore, the efficiency of the model was evaluated using practical indicators and its consistency and accuracy was compared with traditional methods. The performance of the models were assessed using the Dice similarity coefficient (DSC). The Mann-Whitney U test was used to compare continuous clinical variables and the χ^2 test was used for comparisons between categorical clinical variables. T1WI sequences exhibited the optimal performance (training dice: 0.923, testing dice: 0.830, outer validation dice: 0.801), while T2WI showed a relatively poor performance (training dice of 0.761, a testing dice of 0.647, and an outer validation dice of 0.643. In conclusion, the automatic multi-sequences MRI segmentation model for PCNSL in the present study displayed high spatial overlap ratio and similar tumor volume with routine manual segmentation, indicating its significant potential.

Correspondence to: Dr Guang Lu, Department of Hematology, Shandong Second Provincial General Hospital, 4 Duanxing West Road, Huaiyin, Jinan, Shandong 250022, P.R. China
E-mail: luguangshandong@163.com

Dr Weiwei Mou, Department of Pediatrics, Shengli Oilfield Central Hospital, 31 Jinan Road, Dongying, Shandong 257099, P.R. China
E-mail: mouweiwei@126.com

*Contributed equally

Key words: primary central nervous system lymphoma, deep learning model, magnetic resonance imaging, automated segmentations

Introduction

Primary central nervous system lymphoma (PCNSL) is recognized as a distinct category of lymphoma, accounting for ~4% of all brain tumors in the United States (1). In comparison with different lymphoma types, the prognosis for PCNSL is considerably worse, with the 5- and 10-year relative survival rates are 35.2 and 27.5%, respectively (2-4). Furthermore, recent epidemiological data showed a significant rise in PCNSL incidence, reaching 0.4 cases per 100,000 population in 2022 (4), partly due to the aging global population (2,5). Therefore, several deep learning methodologies, enhanced by computer technology, have been utilized in the diagnosis and treatment of numerous cancers, including brain tumors, to transform cancer care (6-8). Despite considerable progress derived from a deeper comprehension of the disease regarding treatment, challenges remain in the management of PCNSL. Only a limited number of studies have used advanced methodologies in their investigation, including our previous research contributions (9-12). This shortage largely stems from the relatively infrequent occurrence of PCNSL, a constrained patient demographic and the high mortality rate associated with PCNSL when compared with other lymphoma types (4,5). Therefore, the present study aimed to contribute meaningfully to tackling the aforementioned challenges.

Magnetic resonance imaging (MRI) using gadolinium-based contrast agents has been used for the detection of PCNSL, serving as the most sensitive imaging modality within radiographic evaluations. Accurate assessment of lesions using

gadolinium-enhanced MRI is essential for planning therapy, monitoring and determining prognosis in PCNSL (13-15), similar to glioma and meningioma. Studies concerning brain tumors, such as glioma and meningioma, have reported that deep learning techniques leveraging MRI can cohesively integrate processes such as medical image fusion, segmentation, feature extraction and classification to effectively classify and segment tumors with marked reproducibility (16,17).

Advancements in computer-aided medicine have notably improved the detection and segmentation of brain tumors using deep learning techniques, facilitating their transition into broader clinical practice (18-20). The implementation of deep learning models for automated tumor detection and segmentation has emerged as a transformative approach, presenting opportunities for integration into long-term treatment monitoring. Nonetheless, achieving precise segmentation of brain lymphoma remains a clinical challenge due to the intricate anatomical features of the tumor and the overlap between the tumor margins and normal brain tissue (21). Moreover, previous findings indicate that standard 2-dimentional (2D) measurements that have traditionally been used to assess tumor size and progression, are not as dependable or accurate as volumetric assessments. Whilst 2D measurements rely on simplified metrics, such as maximum diameter or cross-sectional area, they often fail to capture the complex 3-dimensional (3D) morphology of brain tumors, leading to potential inaccuracies in clinical evaluation and treatment planning (22). Manual segmentation for evaluating brain tumor volumes is labor-intensive and highly susceptible to variability among different raters, resulting in inconsistent interpretations among imaging professionals (22,23). Such inconsistencies can severely affect subsequent evaluations of the disease, treatment choices and monitoring efforts, ultimately impacting the survival and prognosis of patients with PCNSL. Thus, there is a growing need for a segmentation approach that can effectively address the challenges associated with 2D measurements and manual volume assessments. The application of computer-assisted automatic segmentation is regarded as a promising solution, and deep learning enables automated lesion segmentation, reduces variability, enhances throughput and improves the detection of complex lesions.

Currently, deep learning-based approaches dominate the field of medical image segmentation, with U-Net and its variants (including U-Net++, Attention U-Net and 3D U-Net) serving as landmark technologies. These architectures have demonstrated a notable performance in several segmentation tasks, particularly in brain tumors, lung cancer and breast cancer imaging (24). However, despite their clinical potential, these advanced techniques have not been systematically applied to PCNSL segmentation, to the best of our knowledge. Our previous research did not explore the potential of nnU-Net. The limited number of PCNSL cases and the available imaging data have resulted in only a few studies focusing on deep learning models for PCNSL, largely concentrating on differentiating it from other brain tumors, such as glioblastoma (9,10). Moreover, there has been a scarcity of recent investigations applying deep learning for the automatic segmentation of multi-parameter MRI in PCNSL (11). As several studies have reported the effectiveness of automatic segmentation models based on deep learning for specific brain tumors, such as glioma and meningioma, with notable rates of automated detection and precision across several tumor compartments (22,25,26), we hypothesize that these deep learning models could also attain a certain level of accuracy in recognizing and segmenting PCNSL. Consequently, the aim of the present study was to create automated deep learning segmentation models that leverage multi-sequence MRI images as input to reliably detect PCNSL tumors. This method would enable the quantitative calculation of volumes and assess the accuracy and consistency of the outcomes. To address the challenges, the present study used the nnU-Net deep learning framework (27), known for its versatility and effectiveness with limited sample sizes, without requiring manual parameter tuning (28,29).

Materials and methods

Study population. The present retrospective study enrolled patients from the Fifth Medical Center of Chinese PLA General Hospital (Beijing, China), Shengli Oilfield Central Hospital (Dongying, China), Affiliated Hospital of Qingdao University (Qingdao, China), Yantai Yuhuangding Hospital (Yantai, China) and Weifang People's Hospital (Weifang, China). The study was performed according to the principles of the Helsinki Declaration. To ensure consistent ethical standards across all participating institutions, the five hospitals adopted an ethical collaborative review mechanism (lead institution review with participating institution endorsement). The relevant approval documents were provided by Shengli Oilfield Central Hospital and endorsed by the ethics committees of the other four participating institutions (approval no. YX11202401101; March 12, 2024). The ethics committees of the participating hospitals waived the requirement for patient informed consent.

Patients who underwent MRI scans and were initially pathologically diagnosed with PCNSL between September 2016 and March 2022 were recruited. All 53 PCNSL cases identified for the present study were evaluated for the predetermined exclusion and inclusion criteria. These criteria were applied consistently to all patients, regardless of initial or follow-up imaging. The inclusion criteria were as follows: i) Confirmed PCNSL diagnosis by pathology; ii) received treatment at the designated 5 hospitals between September 2016 and March 2022; and iii) completed in-hospital MRI examinations. The exclusion criteria were as follows: i) Extensive leukoencephalopathy (Fazekas III; n=1) (30); ii) severe artifacts (n=1); and iii) absence of an available complete MRI dataset (n=2). The exclusion of patients based on these confounding images was essential for ensuring the accurate representation of tumor morphology and minimizing feature extraction bias during model training. Finally, the cohort consisted of 49 PCNSL who were successfully assessed (Fig. 1).

Image acquisition. All examinations were performed using two MRI scanners: 3T scanner (Siemens Healthineers) and 3T scanner Signa (GE Healthcare), adhered to the standards outlined in the Expert Consensus on MRI Examination Techniques. Contrast-enhanced T1-weighted (T1W) and

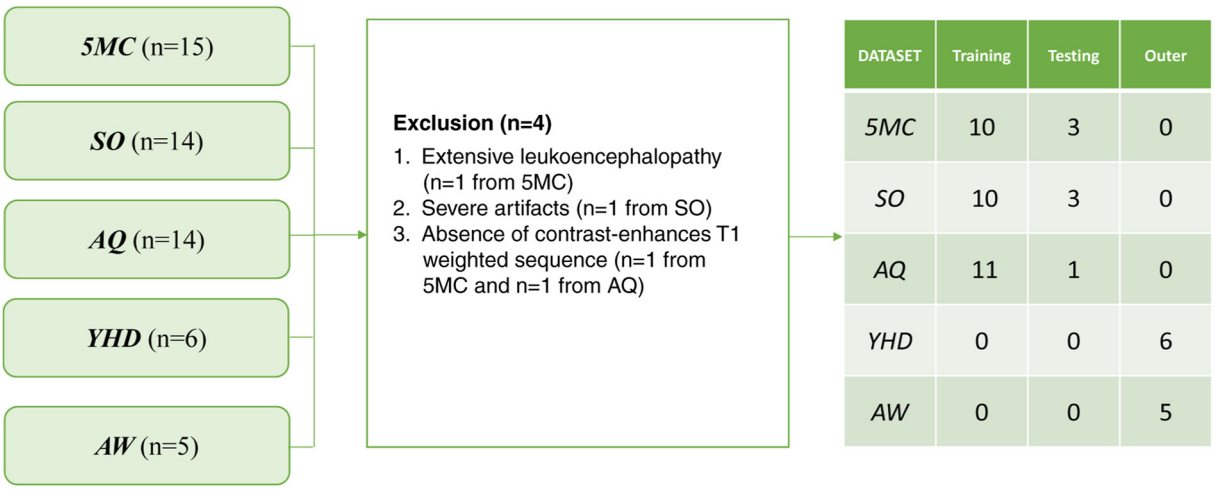

DATASET	Training	Testing	Outer
5MC	10	3	0
SO	10	3	0
AQ	11	1	0
YHD	0	0	6
AW	0	0	5

Figure 1. Cohort of the study. 5MC, The Fifth Medical Center of Chinese PLA General Hospital; SO, Shengli Oilfield Central Hospital; AQ, The Affiliated Hospital of Qingdao University; YHD, Yantai Yuhuangding Hospital; AW, The Affiliated Hospital of Weifang Medical University.

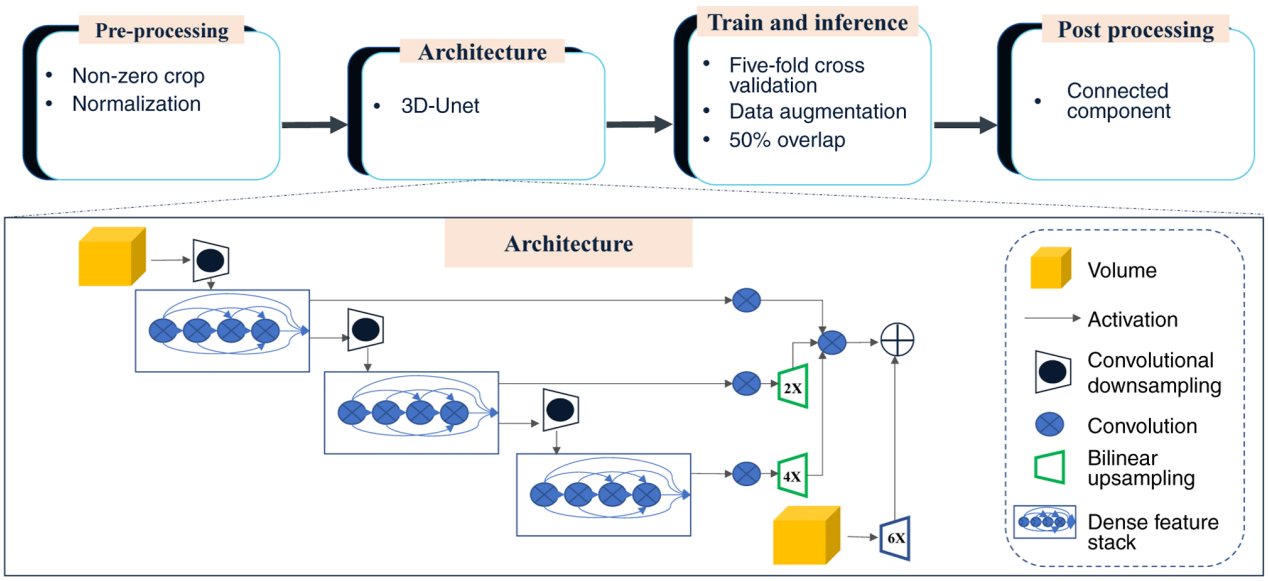

Figure 2. Study workflow and automatic segmentation process overview.

T2-weighted (T2W) images were collected. Gadopentetate dimeglumine was administered intravenously at doses based on the body weight (0.1 mmol/kg). The field of view was set to 256 mm, the matrix was 512x512 and the slice thickness was 5 mm. The images were reconstructed with a standard kernel and then were transferred to an external workstation (syngo MMWP VE 36A; Siemens Healthineers) for further postprocessing.

Image pre-processing. The images were reviewed by a radiologist from Shengli Oilfield Central Hospital with >9 years of experience in radiology, who manually delineated the tumors at the axial site using the Medical Imaging Interaction Toolkit, version 2018.04.2 (www.mitk.org). The marked regions of interest were confirmed as ground truth by another senior neuroradiologist (with 11 years of experience in radiology) from the Fifth Medical Center of Chinese PLA General Hospital, who was blinded to the assessment.

Image segmentation. A total of two segmentation models were established using T1C and T2 scans, respectively. The obtained PCNSL dataset was divided into a training dataset (n=30), a testing dataset (n=8) and an outer validation dataset (n=11). Subsequently, the nnU-Net deep learning network was utilized to train an automated segmentation model (27). nnU-Net framework is an adaptive extension of the conventional U-Net architecture. This innovative framework incorporates automated adaptation mechanisms to accommodate diverse datasets and clinical applications, thereby minimizing manual parameter optimization requirements. The core design philosophy of the framework minimizes unnecessary architectural complexity whilst optimizing essential elements. This approach ensures reliable performance across diverse medical imaging applications while preserving clinical relevance (31). By leveraging nnU-Net, the present study streamlined the key decisions involved in designing an effective segmentation pipeline for the specific dataset. This process is illustrated in Fig. 2.

Table I. Demographic and clinical characteristics of all patients with primary central nervous system lymphoma in the present study (n=49).

Characteristic	Value
Sex	
Male	27 (55.1)
Female	22 (44.9)
Age, years	58.4±9.1
Tumor location	
Telencephalon	37 (75.5)
Thalamus	1 (2.0)
Brainstem	5 (10.2)
Cerebellum	6 (12.2)
History of malignancy	
No	47 (95.9)
Yes	2 (4.1)

Data are presented as mean ± standard deviation or n (%).

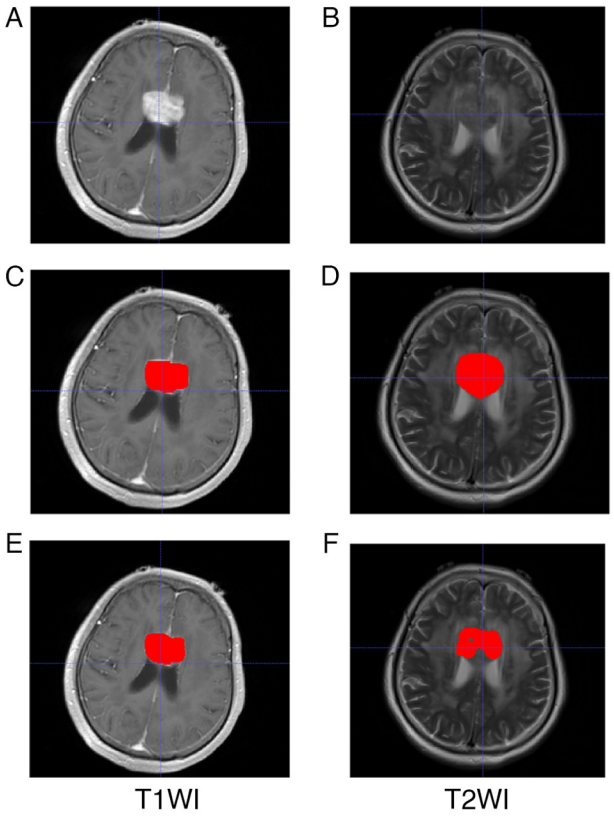

Figure 3. Comparison of two different automated segmentation examples in a 57-year-old female patient. Original (A) T1WI and (B) T2WI sequences. Manually delineated regions of interest as ground truth segmentations are displayed for (C) T1WI and (D) T2WI. The automated segmentation model performance is shown for (E) T1WI and (F) T2WI.

The default framework of nnU-Net was used; however, it was adapted for the characteristics of the data, choosing the 3D fullres model and retaining the original resolution. Preprocessing and data augmentation steps were used to improve classification accuracy before training. To minimize the computational burden and reduce the matrix size, the scans were cropped to the region with non-zero values. The datasets were then resampled to median voxel spacing by utilizing third-order spline interpolation for images and neighbor interpolation for masks. The resampling approach enabled the neural networks to improve the learning of the spatial semantics of the scans. Finally, the entire dataset was normalized by clipping to the (0.5, 99.5) percentile of these intensity values, and the z-score was normalized according to the mean and standard deviation of all collected intensity values in each sample. In the training procedure, the 3D fullres model was used and a combination of dice and cross-entropy loss was utilized according to following formula: $L=L_{crossentropy} + L_{dice}$

The same data augmentation methods were performed to prevent overfitting. The batch size was set adaptively according to video memory. The number of training epochs was 500 at which epoch the model converged. During the training process, 5-fold cross-validation was utilized to optimize computational efficiency and reduce deviation variance. Connected component analysis was used as a postprocessing technique. After inference, the tumors could be segmented automatically.

Statistical analysis. Categorical variables are presented as n (%), whilst continuous variables are summarized as mean ± standard deviation for normally distributed data, or as median (interquartile range) for non-normally data. The Mann-Whitney U test was applied to compare continuous clinical variables, whilst the χ^2 test was used to assess the difference in categorical clinical variables between groups. The Dice similarity coefficient (DSC), which provides a measure of spatial overlap for each voxel of segmented tissue, was used to evaluate the model performance. Volumes of tumor components were calculated and volumetric agreement was evaluated between the ground truth and automated segmentations using the Wilcoxon rank-sum test. Pearson's correlation coefficient (r) was calculated and a Bland-Altman analysis was performed. $P<0.05$ was considered to indicate at statistically significant difference. All statistical analyses were performed using Python (version 3.5.6; Python Software Foundation).

Results

Study population. In the present study, the PCNSL cohort comprised 49 patients (27 men and 22 women) with a mean age of 58.4±9.1 years. The detailed patient demographics of the training and validation sets are presented in Table I. The diagnosis of PCNSL was confirmed through stereotactic biopsy in 40 of the cases and through surgical specimens in 9 of the cases. In addition, systemic lymphatic disease was ruled out by additional imaging and bone marrow biopsy in all cases. The majority of the patients received chemotherapy (91.8%). A total of 93.8% of the PCNSLs were located in the supratentorial region and showed multifocal tumor spread (71.4%).

Evaluation of the segmentation model. The performance results for the segmentation models are outlined in Table II. Compared with the ground truth, the T1WI sequences segmentation model achieved the optimal performance with a training

Table II. Correlation coefficients, dice coefficients and the significant differences in tumor volume between the tumor volumes of the training, testing and outer datasets.

	Correlation coefficient, r		Dice coefficient		P-value	
Dataset	T1WI	T2WI	T1WI	T2WI	T1WI	T2WI
Training	0.76[a]	0.89[a]	0.923	0.761	0.329	0.229
Testing	0.98[a]	0.66[a]	0.830	0.647	0.093	0.779
Outer	0.95[a]	0.98[a]	0.801	0.643	0.013	0.477

[a]P<0.0001.

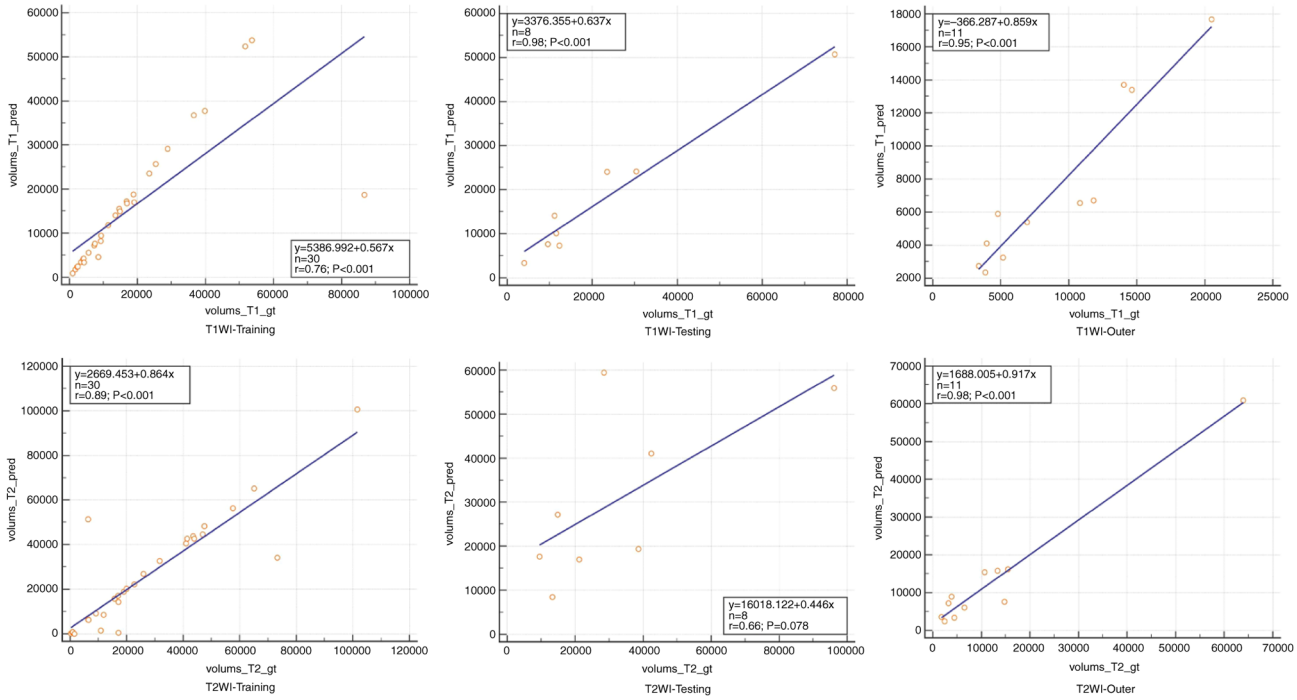

Figure 4. Regression lines for the two segmentation models in the training, testing and outer dataset.

dice of 0.923, a testing dice of 0.830 and an outer validation dice of 0.801. The T1WI sequences model and the T2WI sequences model yielded a mean tumor volume of 15.64±14.26 and 25.77 ± 24.20 cm^3, respectively. Representative images of two different automated segmentation examples from a 57-year-old female patient are shown in Fig. 3.

To compare volumetric assessment by automated segmentations with the ground truth, regression lines for two segmentation models were drawn (Fig. 4). The correlation coefficients for the three models are presented in Table II, which also demonstrates the significant differences in tumor volume between the training, testing and outer datasets. Furthermore, Bland-Altman analysis revealed a good agreement between the manual and automated segmentations (Fig. 5).

Discussion

Precise assessment of size is clinically relevant for therapy planning, prognosis and monitoring in PCNSL. Automated segmentation of PCNSL may enable a precise and objective assessment of tumor burden and response in longitudinal imaging, which is often difficult to determine due to its multifaceted appearance of multiple scattered lesions (22,23). In the present study, two automated segmentation models of PCNSL were established using T1C and T2 scans. The nature of PCNSL tumors generally results in a complex and heterogeneous structure on multiple MRI image sequences. However, the present study observed that the automatic segmentation model demonstrated marked accuracy in its segmentation performance.

The nnU-net-based automated segmentation model in the present study demonstrated a notable performance. Compared with the ground truth, the T1WI sequences segmentation model achieved the optimal performance with a training dice of 0.923, a testing dice of 0.830 and an outer validation dice of 0.801. Bland-Altman analysis revealed high agreement between manual and automated segmentations. Furthermore, both models had strong correlation

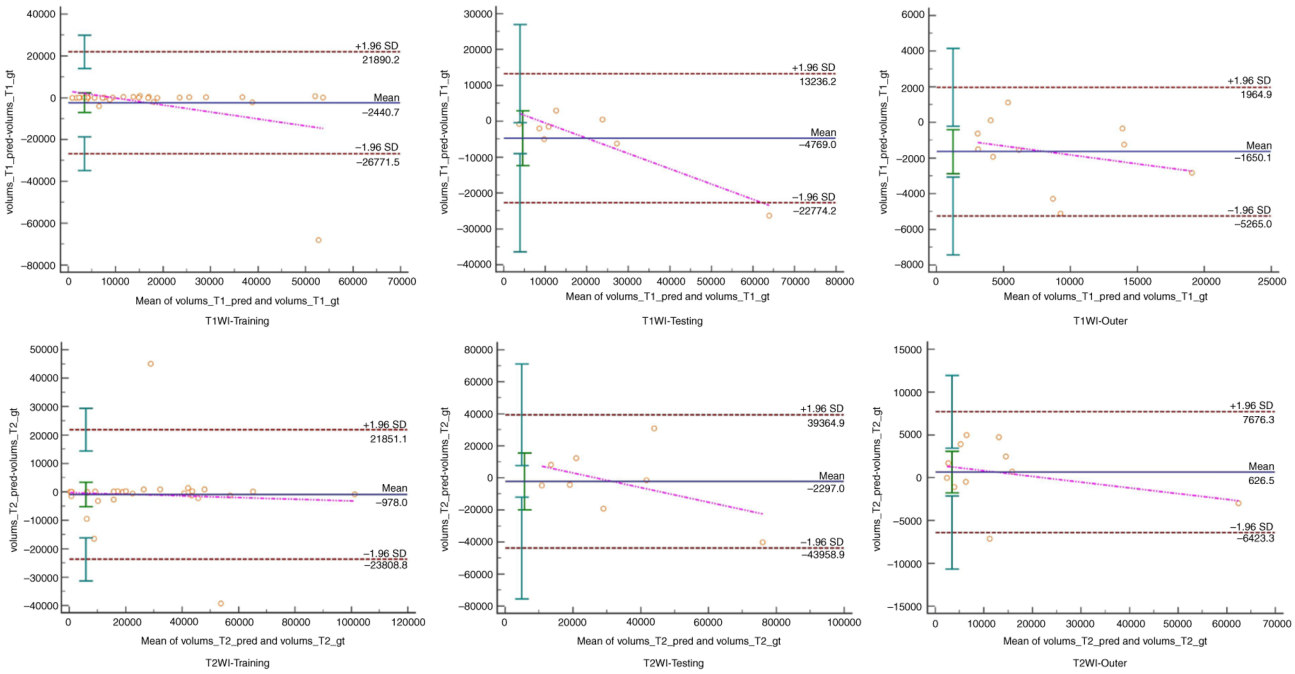

Figure 5. Consistency between manual and automatic segmentation evaluated by Bland-Altman analysis.

coefficient and the automated segmentation architecture was successfully deployed across diverse input data types with ease. Therefore, the deep learning model proposed in the present study is highly clinically relevant as it allows for the automated detection of cerebral masses. This can enable the preselection of lesions and serve as a control mechanism for radiologists and treating physicians.

In comparison with the previously suggested models, the deep learning model in the present study demonstrated superiority. In prior studies, several methods were proposed for glioma, another type of central nervous system tumor, due to similar imaging features and larger glioma datasets. Perkuhn *et al* (32) reported DSCs ranging from 0.62-0.86 for different tumor components of gliomas. This trained segmentation model for gliomas could be successfully applied to PCNSL without any decrease in segmentation performance, despite the different appearance and overall complex structure of PCNSL. Using a different convolutional neural network (CNN), Menze *et al* (33) and Bousabarah *et al* (34) calculated DSCs of 0.74-0.85 and 0.84-0.90 for glioma segmentations, respectively. Kickingereder *et al* (26) reported DSCs of 0.89-0.93 for an artificial neural network trained on a larger cohort of patients with glioblastoma. Pennig *et al* (11) evaluated the efficacy of a deep learning model initially trained on gliomas for fully automated detection and segmentation of PCNSL on multiparametric MRI including heterogeneous imaging data from several scanner vendors and study centers. The median DSC was 0.76 for total tumor volume (11).

CNNs require large annotated datasets for effective training, as small datasets limit generalizability. This is particularly challenging for lymphoma analysis, where variations in lesion size, shape and metabolic activity complicate training without reliable anatomical references. In terms of performance, the present model achieved notable results using only a small sample dataset compared with the previous study (35,36). The T1WI model achieved an improved performance in comparison with the T2WI, and this can be attributed to the improved visualization of tumor morphology on contrast-enhanced T1WI, where tumors typically exhibit distinct homogeneous enhancement patterns (37). Moreover, peritumoral edema appears hyperintense on T2WI, which reflects the infiltration and dissemination of tumor cells along the perivascular space, and is easily confused with the slightly hyperintense signal of the tumor (37). The lower T2WI performance was mainly related to imaging features, rather than model architecture or training bias. Other studies have also reported a similar phenomenon (10,38,39). Therefore, T2WI performance may be improved in the following ways: i) Data enhancement: Improve T2WI data quality through enhancement technology; ii) multimodal fusion: Combine T1WI and T2WI data to improve the segmentation effect; and iii) model optimization: Incorporate a boundary sensing module into the segmentation network to improve the extraction of target boundary features and refine segmentation precision.

The main limitations of the present study include the small sample size and the inherent constraints associated with its retrospective design. Thus, further investigation is needed to determine whether automatic segmentation for PCNSL is suitable for specific clinical tasks and parameters. Despite evaluating the automatic segmentation model using several MRI multi-sequence images from multiple hospital treatment centers, it is essential to acknowledge the potential bias associated with these images. It is also acknowledged that the MRI techniques and learning methods used in the present study could be further optimized. However, at present, acquiring a substantial volume of MRI data from additional patients with PCNSL for external validation remains challenging due to the rarity of this condition. If more PCNSL imaging data become accessible in the future, the performance of the model in the present study could be further optimized. In subsequent studies, the focus should be on compiling a more comprehensive and higher-quality dataset of medical imaging

data for PCNSL, refining the methodology and validating the results in larger, multi-center cohorts to improving the robustness of the model and enhance its potential clinical applicability. The development of brain tumor segmentation methods that can address the issue of missing modalities should also be investigated. Furthermore, data on the prognosis of PCNSL should be collected and the method to form a set of full-process automated diagnosis and treatment solutions for PCNSL should be improved. Although the present research is still in the initial stage, the precise quantification of the lesions will lay a solid foundation for this goal. Furthermore, future studies should perform analyses to explore potential correlations between the artificial intelligence-generated findings (such as tumor segmentation results and predictive scores) and key clinical outcomes, such as treatment response, progression-free survival or overall survival, where data is available. These analyses should aim to establish a stronger link between artificial intelligence findings and clinical outcomes, thereby enhancing the translational value and practical applicability of the model in the present study.

In conclusion, the present study established two automated segmentation models of PCNSL using T1C and T2. Compared with the ground truth, the T1C sequences segmentation model achieved optimal performance. The proposed automatic segmentation model performed well despite the complex and multifaceted appearance of PCNSL. This indicates its great potential for use in the entire follow-up monitoring process for this lymphoma subtype.

Acknowledgements

The authors would like to thank Dr Lixi Miao (Department of Medical Imaging Center, Shengli Oilfield Central Hospital) and Dr Ruyi Tian (Department of Radiology, Fourth Medical Center Chinese PLA General Hospital, Beijing, P.R. China) for assessing the images. Their evaluations provided the essential data foundation for establishing the segmentation model. As doctors from the hospitals that supplied the imaging data, they voluntarily participated in the MRI evaluations but were not involved in any other aspects of this study. In accordance with their wishes and academic standards, they have not been listed as co-authors of this manuscript.

Funding

The present project was funded by the Natural Science Foundation of Dongying, China (grant no. 2023ZR028).

Availability of data and materials

The data generated in the present study may be requested from the corresponding author.

Authors' contributions

TW, XT, JD, and YJ participated in study design and manuscript conceptualization. XT, JD, and YJ participated in study design and manuscript conceptualization. TW developed the model and performed the statistical analysis. GL and XT drafted the work. XT revised the manuscript critically for important intellectual content, provided a discussion of the results and an explanation of the main nnU-Net techniques. JD and YJ submitted ethics applications to five affiliated hospitals; recruited radiologists for manual segmentation of imaging data and coordinated with co-authors to distribute workloads. JD and YJ confirm the authenticity of all the raw data. GL and WM contributed to the conception of the work and oversaw project progress while ensuring workflow execution. All authors read and approved the final manuscript.

Ethics approval and consent to participate

The present retrospective study was performed in compliance with the Helsinki Declaration and was approved by the Independent Ethics Committees of the Fifth Medical Center of Chinese PLA General Hospital, the Affiliated Hospital of Qingdao University, Yantai Yuhuangding Hospital, Weifang People's Hospital and Shengli Oilfield Central Hospital (March 12, 2024; approval no. YX11202401101). The ethics committees waived the requirement for obtaining informed consent from patients.

Patient consent for publication

The patient provided written informed consent for the publication of any data and/or accompanying images.

Competing interests

The authors declare that they have no competing interests.

References

1. Villano JL, Shaikh H, Dolecek TA and McCarthy BJ: Age, gender, and racial differences in incidence and survival in primary CNS lymphoma. Br J Cancer 105: 1414-1418, 2011.
2. Chukwueke U, Grommes C and Nayak L: Primary central nervous system lymphomas. Hematol Oncol Clin North Am 36: 147-159, 2022.
3. Morales-Martinez A, Nichelli L, Hernandez-Verdin I, Houillier C, Alentorn A and Hoang-Xuan K: Prognostic factors in primary central nervous system lymphoma. Curr Opin Oncol 34: 676-684, 2022.
4. Schaff LR and Grommes C: Primary central nervous system lymphoma. Blood 140: 971-979, 2022.
5. Lukas RV, Stupp R, Gondi V and Raizer JJ: Primary central nervous system Lymphoma-PART 1: Epidemiology, diagnosis, staging, and prognosis. Oncology (Williston Park) 32: 17-22, 2018.
6. Sangeetha SKB, Muthukumaran V, Deeba K, Rajadurai H, Maheshwari V and Dalu GT: Multiconvolutional transfer learning for 3D brain tumor magnetic resonance images. Comput Intell Neurosci 2022: 8722476, 2022.
7. Sadad T, Rehman A, Munir A, Saba T, Tariq U, Ayesha N and Abbasi R: Brain tumor detection and multi-classification using advanced deep learning techniques. Microsc Res Tech 84: 1296-1308, 2021.
8. Abd-Ellah MK, Awad AI, Khalaf AAM and Hamed HFA: A review on brain tumor diagnosis from MRI images: Practical implications, key achievements, and lessons learned. Magn Reson Imaging 61: 300-318, 2019.
9. Lu G, Zhang Y, Wang W, Miao L and Mou W: Machine learning and deep learning CT-based models for predicting the primary central nervous system lymphoma and glioma types: A multicenter retrospective study. Front Neurol 13: 905227, 2022.
10. Xia W, Hu B, Li H, Shi W, Tang Y, Yu Y, Geng C, Wu Q, Yang L, Yu Z, *et al*: Deep learning for automatic differential diagnosis of primary central nervous system lymphoma and glioblastoma: Multi-parametric magnetic resonance imaging based convolutional neural network model. J Magn Reson Imaging 54: 880-887, 2021.

11. Pennig L, Hoyer UCI, Goertz L, Shahzad R, Persigehl T, Thiele F, Perkuhn M, Ruge MI, Kabbasch C, Borggrefe J, *et al*: Primary central nervous system lymphoma: Clinical evaluation of automated segmentation on multiparametric MRI using deep learning. J Magn Reson Imaging 53: 259-268, 2021.
12. Ramadan S, Radice T, Ismail A, Fiori S and Tarella C: Advances in therapeutic strategies for primary CNS B-cell lymphomas. Expert Rev Hematol 15: 295-304, 2022.
13. Batchelor TT: Primary central nervous system lymphoma. Hematology Am Soc Hematol Educ Program 2016: 379-385, 2016.
14. Bonm AV, Ritterbusch R, Throckmorton P and Graber JJ: Clinical imaging for diagnostic challenges in the management of gliomas: A review. J Neuroimaging 30: 139-145, 2020.
15. Huang RY, Bi WL, Griffith B, Kaufmann TJ, la Fougère C, Schmidt NO, Tonn JC, Vogelbaum MA, Wen PY, Aldape K, *et al*: Imaging and diagnostic advances for intracranial meningiomas. Neuro Oncol 21: i44-i61, 2019.
16. Yadav AS, Kumar S, Karetla GR, Cotrina-Aliaga JC, Arias-Gonzáles JL, Kumar V, Srivastava S, Gupta R, Ibrahim S, Paul R, *et al*: A feature extraction using probabilistic neural network and BTFSC-Net model with deep learning for brain tumor classification. J Imaging 9: 10, 2022.
17. ZainEldin H, Gamel SA, El-Kenawy EM, Alharbi AH, Khafaga DS, Ibrahim A and Talaat FM: Brain tumor detection and classification using deep learning and Sine-cosine fitness grey wolf optimization. Bioengineering (Basel) 10: 18, 2022.
18. Taher F, Shoaib MR, Emara HM, Abdelwahab KM, Abd El-Samie FE and Haweel MT: Efficient framework for brain tumor detection using different deep learning techniques. Front Public Health 10: 959667, 2022.
19. Hwang K, Park J, Kwon YJ, Cho SJ, Choi BS, Kim J, Kim E, Jang J, Ahn KS, Kim S and Kim CY: Fully automated segmentation models of supratentorial meningiomas assisted by inclusion of normal brain images. J Imaging 8: 327, 2022.
20. Dang K, Vo T, Ngo L and Ha H: A deep learning framework integrating MRI image preprocessing methods for brain tumor segmentation and classification. IBRO Neurosci Rep 13: 523-532, 2022.
21. Lin YY, Guo WY, Lu CF, Peng SJ, Wu YT and Lee CC: Application of artificial intelligence to stereotactic radiosurgery for intracranial lesions: Detection, segmentation, and outcome prediction. J Neurooncol 161: 441-450, 2023.
22. Laukamp KR, Pennig L, Thiele F, Reimer R, Görtz L, Shakirin G, Zopfs D, Timmer M, Perkuhn M and Borggrefe J: Automated meningioma segmentation in multiparametric MRI: comparable effectiveness of a deep learning model and manual segmentation. Clin Neuroradiol 31: 357-366, 2021.
23. Chang K, Beers AL, Bai HX, Brown JM, Ly KI, Li X, Senders JT, Kavouridis VK, Boaro A, Su C, *et al*: Automatic assessment of glioma burden: A deep learning algorithm for fully automated volumetric and bidimensional measurement. Neuro Oncol 21: 1412-1422, 2019.
24. Peng J, Luo H, Zhao G, Lin C, Yi X and Chen S: A Review of medical image segmentation algorithms based on deep learning. Computer Engineering Appl 57: 44-57, 2021 (In Chinese).
25. Latif G: DeepTumor: Framework for brain MR image classification, segmentation and tumor detection. Diagnostics (Basel) 12: 2888, 2022.
26. Kickingereder P, Isensee F, Tursunova I, Petersen J, Neuberger U, Bonekamp D, Brugnara G, Schell M, Kessler T, Foltyn M, *et al*: Automated quantitative tumour response assessment of MRI in neuro-oncology with artificial neural networks: A multicentre, retrospective study. Lancet Oncol 20: 728-740, 2019.
27. Isensee F, Jaeger PF, Kohl SAA, Petersen J and Maier-Hein KH: nnU-Net: A self-configuring method for deep learning-based biomedical image segmentation. Nat Methods 18: 203-211, 2021.
28. Pemberton HG, Wu J, Kommers I, Müller DMJ, Hu Y, Goodkin O, Vos SB, Bisdas S, Robe PA, Ardon H, *et al*: Multi-class glioma segmentation on real-world data with missing MRI sequences: Comparison of three deep learning algorithms. Sci Rep 13: 18911, 2023.
29. Ganesan P, Feng R, Deb B, Tjong FVY, Rogers AJ, Ruipérez-Campillo S, Somani S, Clopton P, Baykaner T, Rodrigo M, *et al*: Novel domain Knowledge-encoding algorithm enables Label-efficient deep learning for cardiac CT segmentation to guide atrial fibrillation treatment in a pilot dataset. Diagnostics (Basel) 14: 1538, 2024.
30. Fazekas F, Chawluk JB, Alavi A, Hurtig HI and Zimmerman RA: MR signal abnormalities at 1.5 T in Alzheimer's dementia and normal aging. AJR Am J Roentgenol 149: 351-356, 1987.
31. Isensee F, Petersen J, Klein A, Zimmerer D, Jaeger PF, Kohl S, Wasserthal J, Koehler G, Norajitra T, Wirkert S and Maier-Hein KH: nnU-Net: Self-adapting framework for U-Net-based medical image segmentation. ArXiv abs/1809.10486, 2018.
32. Perkuhn M, Stavrinou P, Thiele F, Shakirin G, Mohan M, Garmpis D, Kabbasch C and Borggrefe J: Clinical evaluation of a multiparametric deep learning model for glioblastoma segmentation using heterogeneous magnetic resonance imaging data from clinical routine. Invest Radiol 53: 647-654, 2018.
33. Menze BH, Jakab A, Bauer S, Kalpathy-Cramer J, Farahani K, Kirby J, Burren Y, Porz N, Slotboom J, Wiest R, *et al*: The multimodal brain tumor image segmentation benchmark (BRATS). IEEE Trans Med Imaging 34: 1993-2024, 2015.
34. Bousabarah K, Letzen B, Tefera J, Savic L, Schobert I, Schlachter T, Staib LH, Kocher M, Chapiro J and Lin M: Automated detection and delineation of hepatocellular carcinoma on multiphasic contrast-enhanced MRI using deep learning. Abdom Radiol (NY) 46: 216-225, 2021.
35. Naser PV, Maurer MC, Fischer M, Karimian-Jazi K, Ben-Salah C, Bajwa AA, Jakobs M, Jungk C, Jesser J, Bendszus M, *et al*: Deep learning aided preoperative diagnosis of primary central nervous system lymphoma. iScience 27: 109023, 2024.
36. Cassinelli Petersen GI, Shatalov J, Verma T, Brim WR, Subramanian H, Brackett A, Bahar RC, Merkaj S, Zeevi T, Staib LH, *et al*: Machine learning in differentiating gliomas from primary CNS lymphomas: A systematic review, reporting quality, and risk of bias assessment. AJNR Am J Neuroradiol 43: 526-533, 2022.
37. Ferreri AJM, Calimeri T, Cwynarski K, Dietrich J, Grommes C, Hoang-Xuan K, Hu LS, Illerhaus G, Nayak L, Ponzoni M and Batchelor TT: Primary central nervous system lymphoma. Nat Rev Dis Primers 9: 29, 2023.
38. Gill CM, Loewenstern J, Rutland JW, Arib H, Pain M, Umphlett M, Kinoshita Y, McBride RB, Bederson J, Donovan M, *et al*: Peritumoral edema correlates with mutational burden in meningiomas. Neuroradiology 63: 73-80, 2021
39. Reszec J, Hermanowicz A, Rutkowski R, Turek G, Mariak Z and Chyczewski L: Expression of MMP-9 and VEGF in meningiomas and their correlation with peritumoral brain edema. Biomed Res Int 2015: 646853, 2015.